Introduction to Color Doppler Ultrasound of the Skin

1

Diana Gaitini

A comprehensive review of the basics of ultrasound focused on the requisites for skin, nail and scalp examinations

Contents

1.1 Introduction

Ultrasound has become a unique medical imaging tool in the investigation of dermatological diseases. By providing high-resolution gray scale images and blood flow information in real time, ultrasound can provide detailed anatomic and physiologic data of skin lesions and deeper soft-tissue changes. Lesion size in three dimensions-lengths, width and depth, morphology, inner structure -solid, cystic or mixed, homogeneous or inhomogeneous, foci of calcifications or necrosis, location, and extension can be diagnosed. By defining vascularity in real time, color and spectral Doppler ultrasound have been proven useful in the study of localized lesions of the skin. Interventional procedures such as tumor biopsy, collection drainage, foreign body removement, and needle localization of lesions can safely be performed under ultrasound guidance. The detailed anatomic information provided by sonography is useful in planning surgery. Magnetic resonance imaging (MRI) is frequently recommended for preoperative assessment although it requires the use of intravenous contrast media and can be less efficient in detecting tumors <3 mm in diameter. Ultrasound is a non-invasive and non-radiating test and as so, follow-up examinations can be performed without potential radiation damage. Finally, operator skills and knowledge of the clinical setting and the question being asked are important in ultrasound success.

1.2 Technical Considerations

Modern digital ultrasound systems utilize *transducers* with a broad range of frequencies (broad bandwidth) [1]. High variable-frequency ultrasound (HVFUS) ranging from 6 to 18 MHz with a Doppler frequency ranging from 7 to 4 MHz is a recently available technique capable of clearly defining skin layers and deeper structures as well as vascularization patterns in real time (Fig. 1.1). With a wide array of frequency availability and adjustable focus, echo sources at different depths can be accurately pinpointed. Small footprint light-weight

D. Gaitini, MD
Unit of Ultrasound, Department of Medical Imaging,
Rambam Health Care Campus,
Ha'alya Ha'shnia 8, Haifa 31096, Israel

Ruth and Bruce Rappaport Faculty of Medicine,
Technion – Israel Institute of Technology, Haifa, Israel
e-mail: d_gaitini@rambam.health.gov.il

X. Wortsman, G.B.E. Jemec (eds.), *Dermatologic Ultrasound with Clinical and Histologic Correlations*,
DOI 10.1007/978-1-4614-7184-4_1,

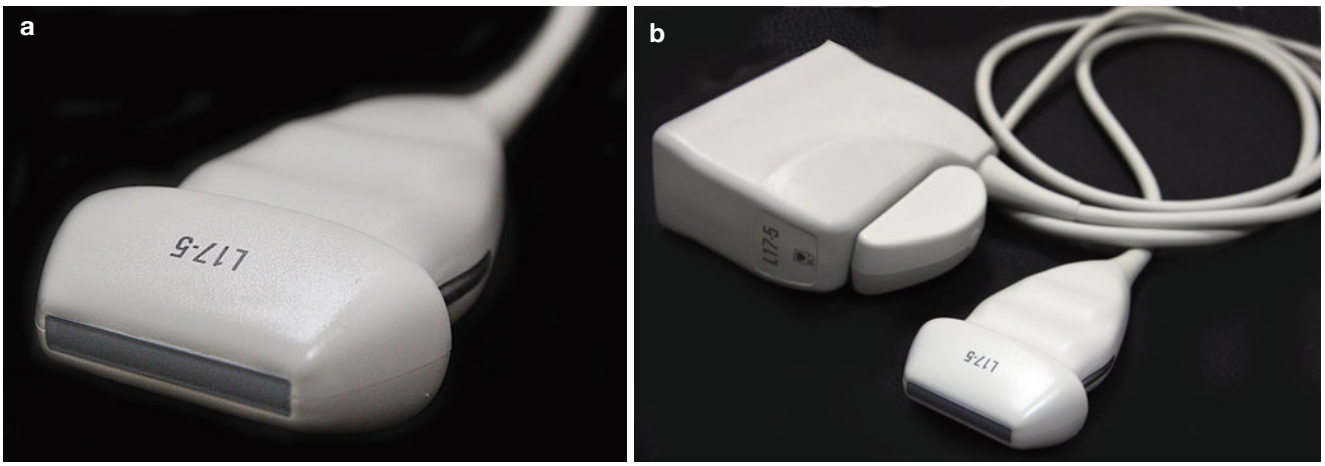

Fig. 1.1 HVFUS linear array transducer. (**a**, **b**) High-resolution (5.0–17.0 MHz) transducers are used for superficial applications: small parts, breast, superficial vascular, and musculoskeletal including skin

Fig. 1.2 HVFUS linear array "hockey stick" transducer. Versatile multi-frequency (up to 15 Mhz) compact 'hockey stick'-shape transducer, with a high Doppler and color flow sensitivity. The hockey stick-shape allows complete contact with the skin surface, reducing scattering artifacts, making it a good choice for superficial and vascular imaging

7–15 MHz linear array probes of compact "hockey stick" shape (Fig. 1.2) allow complete contact with the skin surface, reducing scattering *artifacts*. Hockey stick probes allow better access to mobile structures such as the tongue, or small appendixes such as children's fingers. Fixed (nonvariable) high-frequency ultrasound transducers are activated at a single high operating frequency (20–100 MHz) that determines both *resolution* and the depth of penetration (6–7 mm at 20 MHz; 3 mm at 75 MHz). Most lesions examined in skin ultrasound involve subepidermal structures that would be out of reach for devices of low penetrating power. Furthermore, images produced by fixed high-frequency ultrasound transducers are more pixeled. Deep subcutaneous tissues are not shown and real-time data on blood flow and vascular pattern are lacking [2–5]. In vivo confocal laser microscopy, another imaging technique, has a low penetration of only 0.5 mm, which limits its applicability to lesions of epidermis and papillary dermis [6]. Other imaging techniques such as MRI or positron emission tomography/computed tomography (PET-CT) have limited spatial resolution allowing definition of skin lesions only when greater than 5 mm. MRI and PET-CT require an intravenously administered contrast medium, are more expensive, and less available [7]. In comparison, HVFUS can define lesions in the submillimeter range (down to 0.1 mm). It can reach depths of 60 mm using a single probe with combinations of variable frequencies (7–15 MHz). Ultrasound using frequencies of 15 MHz or higher can clearly define skin layers morphology including changes in epidermal thickness. Although in its current version, ultrasound cannot detect lesions that are epidermal only or that measure less than 0.1 mm in depth. Adjustments of focus at a selected depth and selection of the transmission frequency provide a complete view of the skin and the deeper structures (muscles, tendons, and bone margins), with minimal dispersion of the sound energy waves. Frequencies in the upper range (14–15 MHz) are used for skin layer demonstrations and frequencies in the lower range (7–13 MHz) for the deeper tissues. The resulting composite imaging therefore integrates the effects of frequency-specific tissue reflectance

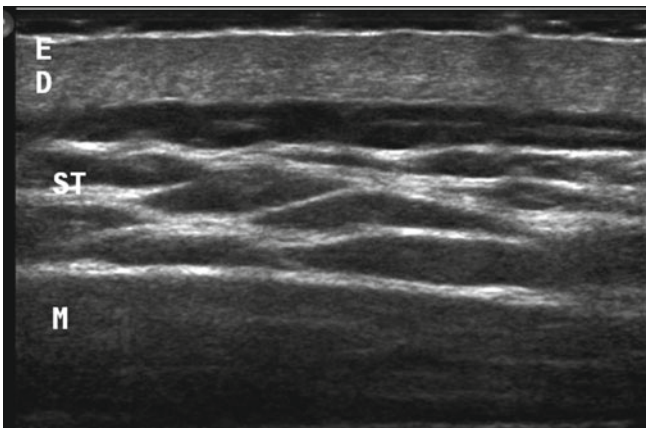

Fig. 1.3 HVFUS image of skin layers and deeper structures. Adjustments of focus at a selected depth and selection of the transmission frequency provide a complete view of the skin and the deeper structures Frequencies in the upper range (14–15 MHz) are used for skin layers and frequencies in the lower range (7–13 MHz) for the deeper tissues demonstration. *E* epidermis, *D* dermis, *ST* subcutaneous tissue, *M* muscle

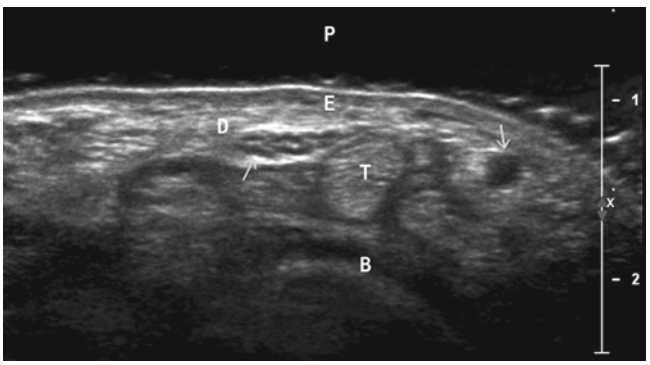

Fig. 1.4 HVFUS image of superficial structures. Axial scan at the level of the wrist. Variable frequency gives the best balance among spatial resolution and depth (2 cm penetration in this scan), generating good quality images of the skin (*E* epidermis, *D* dermis), tendons (*T*), and bone (*B*). Subcutaneous venous and arterial blood vessels appear as echofree ducts (*upper arrow*, ulnar artery). Nerves are seen as small hypoechoic dots surrounded by hyperechogenic tissue (*lower arrow*, median nerve). A gel pad (*P*) was interposed between the transducer and the skin, to reduce near field artifacts

and full-field automatic scanning. The images produced are sharp, obtained in real time, and provide quantitative estimation of blood flow. Thus, of all the imaging techniques available, HVFUS gives the best balance among spatial resolution, depth, and costs generating good quality images of all skin layers, muscles, tendons, and nerves (Fig. 1.3). Ultrasound examination is largely operator dependent – the quality of the obtained information depends mostly on the skill and experience of the examiner. Optimal adjustments of the technical settings are needed in every ultrasound scan. A good amount of gel over the skin is recommended to avoid artifacts from near field (Fig. 1.4). The operator should avoid pressing with the transducer because that may result in disappearing or false thinning of lesions.

Modern equipment software includes capabilities for *harmonic* imaging, *compound* image, extended field of view (EFOV), and *3-D ultrasound*. Tissue harmonic imaging reduces imaging artifacts caused by the interaction of the ultrasound beam with superficial structures or from aberrations at the edges of the beam profile. The artifact-producing signals are of low energy, insufficient to generate harmonic frequencies. Images generated exhibit reduced noise and improved spatial resolution (Fig. 1.5). Spatial compounding improves significant the contrast-to-noise ratio by reducing artifacts generated by the scattering of ultrasound from small tissue reflectors (speckle) [8] (Fig. 1.6). Extended EFOV allows acquisition and display of a panoramic image offering the possibility of viewing topographic anatomic structures with no loss in resolution [9] (Figs. 1.7 and 1.8). Three-dimensional (3D) imaging permits volume data to be displayed in multiple planes and allows accurate measurement of lesion volume.

High-resolution ultrasound imaging of normal skin shows a clear separation of skin layers [10]. The epidermis is seen as a thin *hyperechoic* line. In the palmar and plantar areas, the epidermis is thicker and bilaminar. The dermis is seen as a hyperechoic band of variable thickness, thin in the forearm and thicker in the lumbar region because of its high collagen content. The subcutaneous tissue is *hypoechoic*, generated by fat lobules, which are surrounded by hyperechoic fibrous septa. Subcutaneous venous and arterial blood vessels appear as thin *echo free* ducts. The bone margin appears as a distinct hyperechoic line (Fig. 1.9). The nail plates appear as two hyperechoic parallel lines. The nail bed and the matrix zone are hypoechoic – the matrix is slightly more hypoechoic than the proximal nail bed – contrasting with the hyperechogenicity of the overlying dermis (Fig. 1.10). On the ultrasound examination of healthy individuals, the epidermis shows a laminar hyperechoic appearance provided by the higher amount of keratin in this layer, and a mean epidermal thickness of 0.6 mm (SD 0.8–0.1 mm); normal plantar dermis appears as a hyperechoic band resulting from the higher presence of collagen, with a mean thickness of 1.1 mm. The subcutaneous tissue is a hypoechoic structure provided by fat lobules separated by hyperechoic fibrous septa. Blood flow is predominantly produced by thin (<1 mm) and easily compressible venous vessels in the subcutaneous tissue. No significant arterial vessels in the dermis are detected in healthy subjects.

The ability of sonography to show and characterize even minimal morphostructure was enhanced by the development of Doppler sonography [1]. Doppler ultrasound allows blood flow detection and definition of flow direction, characteristics, and velocity. The reflected ultrasound from a stationary target has the same frequency as the transmitted sound. Oppositely, the reflected sound from a moving target has a different frequency from the transmitted sound. The *Doppler effect* reflects the change in frequency and is directly propor-

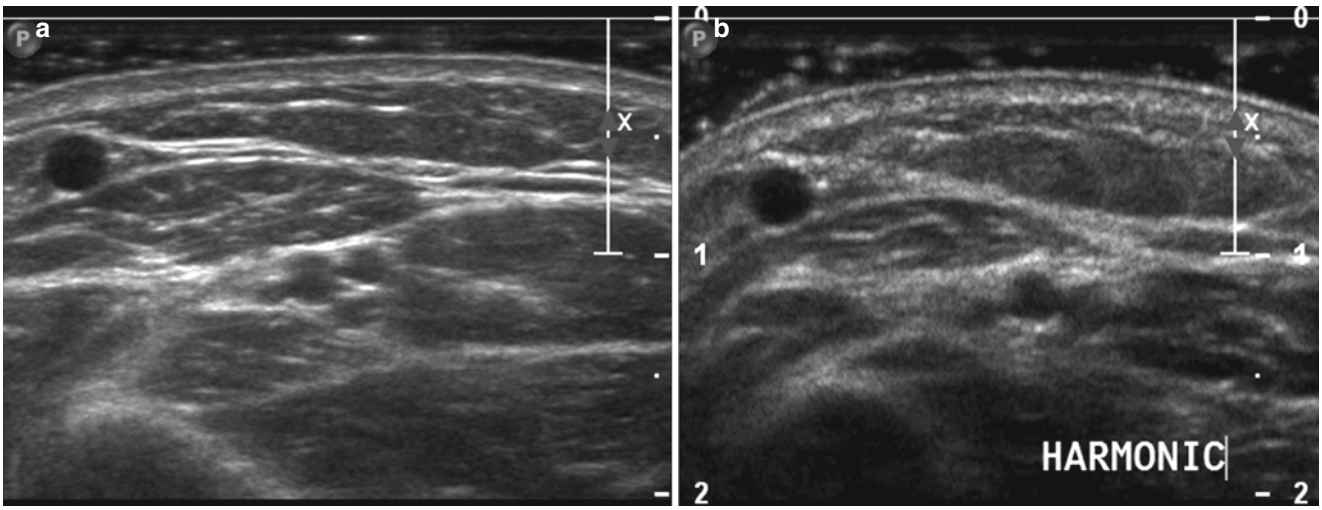

Fig. 1.5 (a,b) Harmonic tissue imaging. Split image at the same anatomic area (**a**) Compound scan. (**b**) Harmonic imaging. Harmonic imaging reduces near-field artifacts, caused by the interaction of the ultrasound beam with superficial structures. The generated images exhibit reduced noise and improved spatial resolution

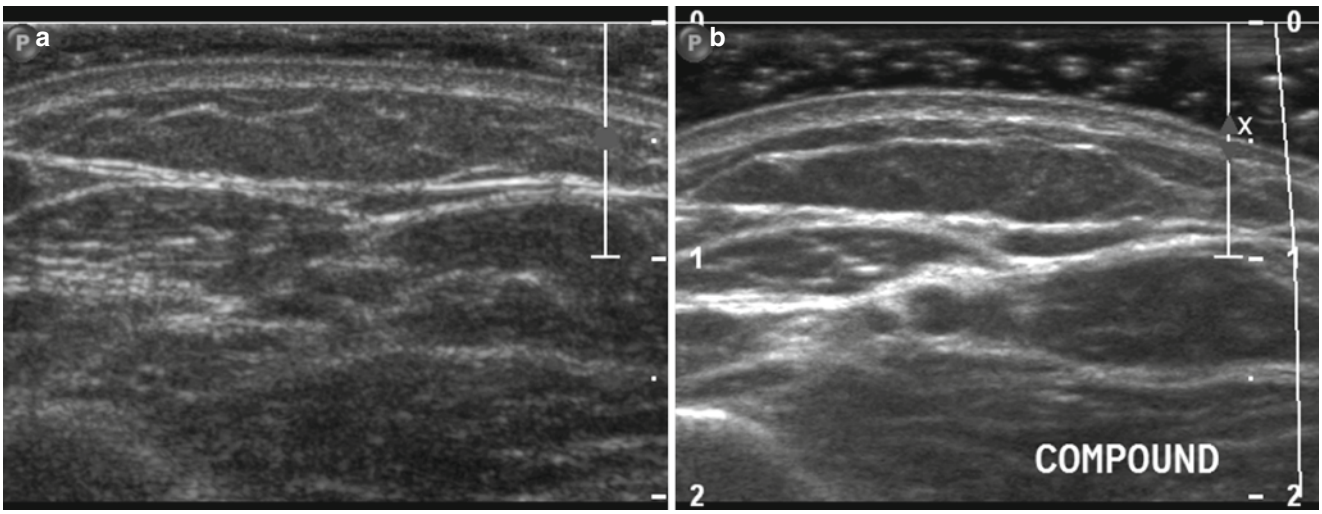

Fig. 1.6 (a, b) Spatial compounding imaging. Split image at the same anatomic area (**a**) Fundamental scan. (**b**) Compounding imaging. Compound significantly improves contrast-to-noise ratio by reducing artifacts generated by the scattering of ultrasound from small tissue reflectors (speckle)

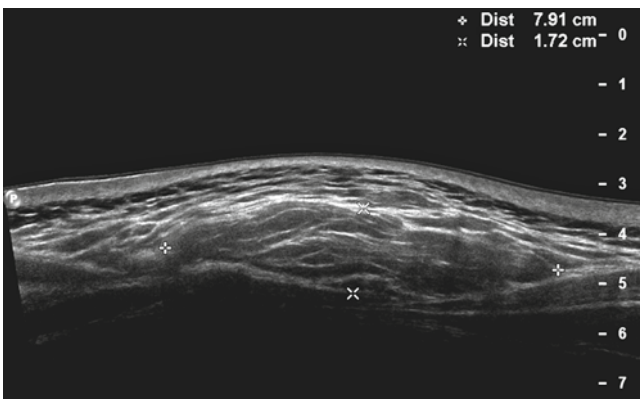

Fig. 1.7 Extended field of view (EFOV) imaging. EFOV−also termed panoramic view (*P* in left image corner)−allows acquisition and display of a panoramic image of large structures and the topographic anatomic relationships with the surrounding tissues, with no loss in resolution. In this case, an oval lesion in the subcutaneous tissue is seen, measuring 7.9 cm in length, compatible with a subcutaneous lipoma

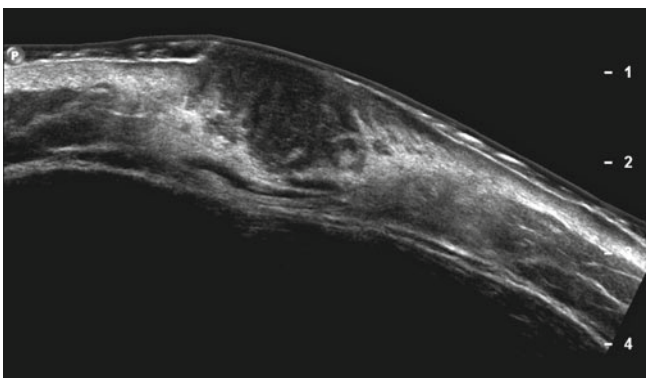

Fig. 1.8 Panoramic (EFOV) view. A malignant skin lesion (dermatofibrosarcoma) is presented. The tumor is hypoechogenic and poorly delimitated. Panoramic imaging shows lesion extension into the epidermis, dermis, and subcutaneous fat tissue

tional to the velocity of the moving target. Accurate estimation of target velocity requires precise measurement of the Doppler frequency shift and angle of insonation of the target in movement. Doppler measurements must be made at less than or equal to 60° the angle of insonation. Because the cosine of the angle changes rapidly for larger angles, and at an angle of 90° there is no relative movement of the target toward or away from the transducer, therefore no Doppler shift is detected. As Doppler frequency shifts fall in the audible range, the heard signal may provide information about flow characteristics. Doppler shifts can be displayed in graphic forms (Doppler frequency spectrum) and in color (color flow and power mode Doppler) (Fig. 1.11). The Doppler frequency spectrum shows changes in flow velocity and direction by vertical deflections of the waveform above and below the baseline. Doppler parameters such as maximum systolic, minimum diastolic, and mean blood flow velocity and the *pulsatility and the resistive indices* can be calculated (Fig. 1.12). Color flow imaging displays flowing blood in a color map, superimposed on the gray-scale image in real time. Color flow is able to provide flow direction (red towards the transducer, blue away from the transducer) and relative velocity information (lighter hues corresponding to higher velocities). Power mode uses a single color map to display the power or amplitude of the Doppler signals. Power mode has increased sensitivity for flow detection, but lacks information on flow direction and flow velocity. Low velocity flow and poorly vascularized lesions in the skin are better displayed by power Doppler. Color Doppler provides better information in higher flow velocity and hypervascular lesions, demonstrating flow direction and relative velocities. On color Doppler mode, color artifacts may be reduced to a minimum by optimizing the color Doppler amplification, degrading it until only pulsating color pixels are left. Absence of intralesion vessels may be proved by increasing Doppler amplification until many colored artifacts are seen around the lesion. Spectral Doppler display allows differentiation between venous and arterial flow. Flow velocity measurements and flow characteristics may be obtained (Fig. 1.13). Combining gray scale ultrasound with Doppler ultrasound, accurate definition of skin lesions features may be obtained, including internal echogenicity, size, shape, margins, skin layers involvement and blood flow (Fig. 1.14). Sonography may be useful to differentiate between inflammation, vascular lesions, and tumors. Increased dermal thickness (mean ± SD, 3.3 ± 1.0 mm vs. 1.4 ± 0.3 mm for normal individuals) allowed identifying subclinical lesions and the extension of lesions into clinically normal looking skin. Modern high-resolution equipments using high-frequency probes and a very sensitive power Doppler technique allows a clear definition of the cutaneous and muscular layers, as well as vascularity of skin and

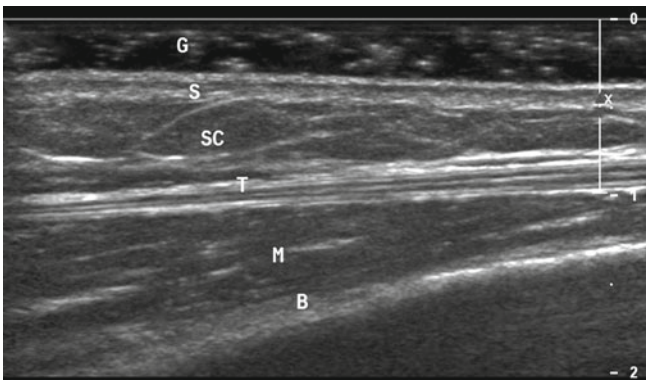

Fig. 1.9 High-resolution ultrasound image of normal skin and deeper structures. Longitudinal scan at the level of the forearm. A clear separation of skin layers (*S*) is shown. The epidermis is seen as a thin hyperechoic line. The dermis is seen as a hyperechoic band of variable thickness, thin in the forearm and thicker in the lumbar region because of a high collagen content. The subcutaneous tissue (*SC*) is hypoechoic, generated by fat lobules, which are surrounded by hyperechoic fibrous septa. Tendons (*T*) are hyperechogenic with parallel hypoechogenic lines. Muscles (*M*) are hypoechogenic, with parallel echogenic lines. The bone margin (*B*) appears as a distinct hyperechoic line. The focus is adjusted at the superficial level (*vertical line* on the right side of the image), to allow better definition of the skin. A good amount of gel (*G*) over the skin is recommended in order to avoid near-field artifacts

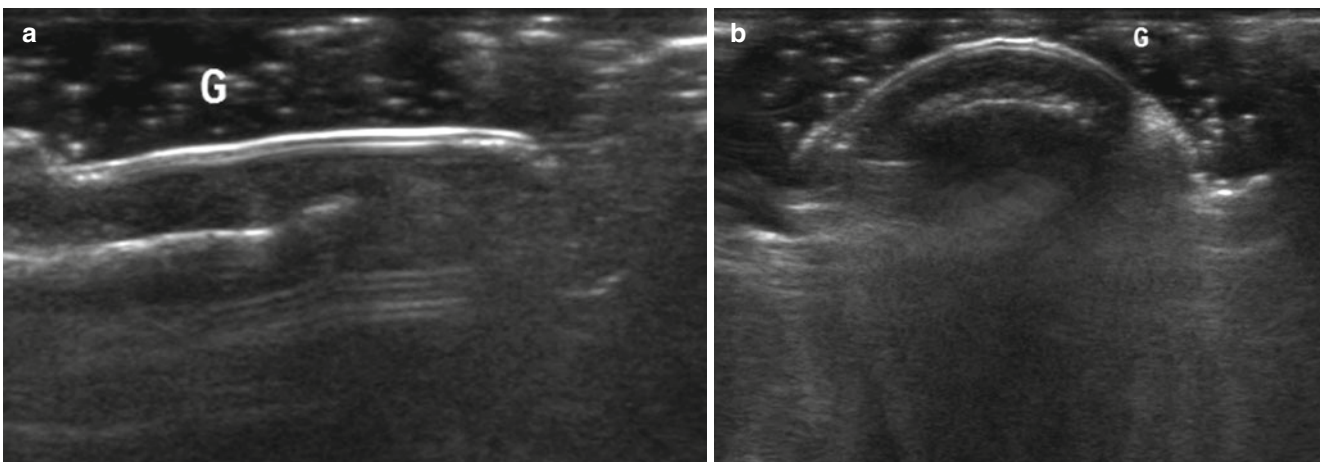

Fig. 1.10 High resolution US of the nail. (**a**) Longitudinal view. (**b**) Transverse view. The nail plates appear as two hyperechoic parallel lines. The nail bed and the matrix zone below the plates are hypoechoic. *G* gel spread over the nail

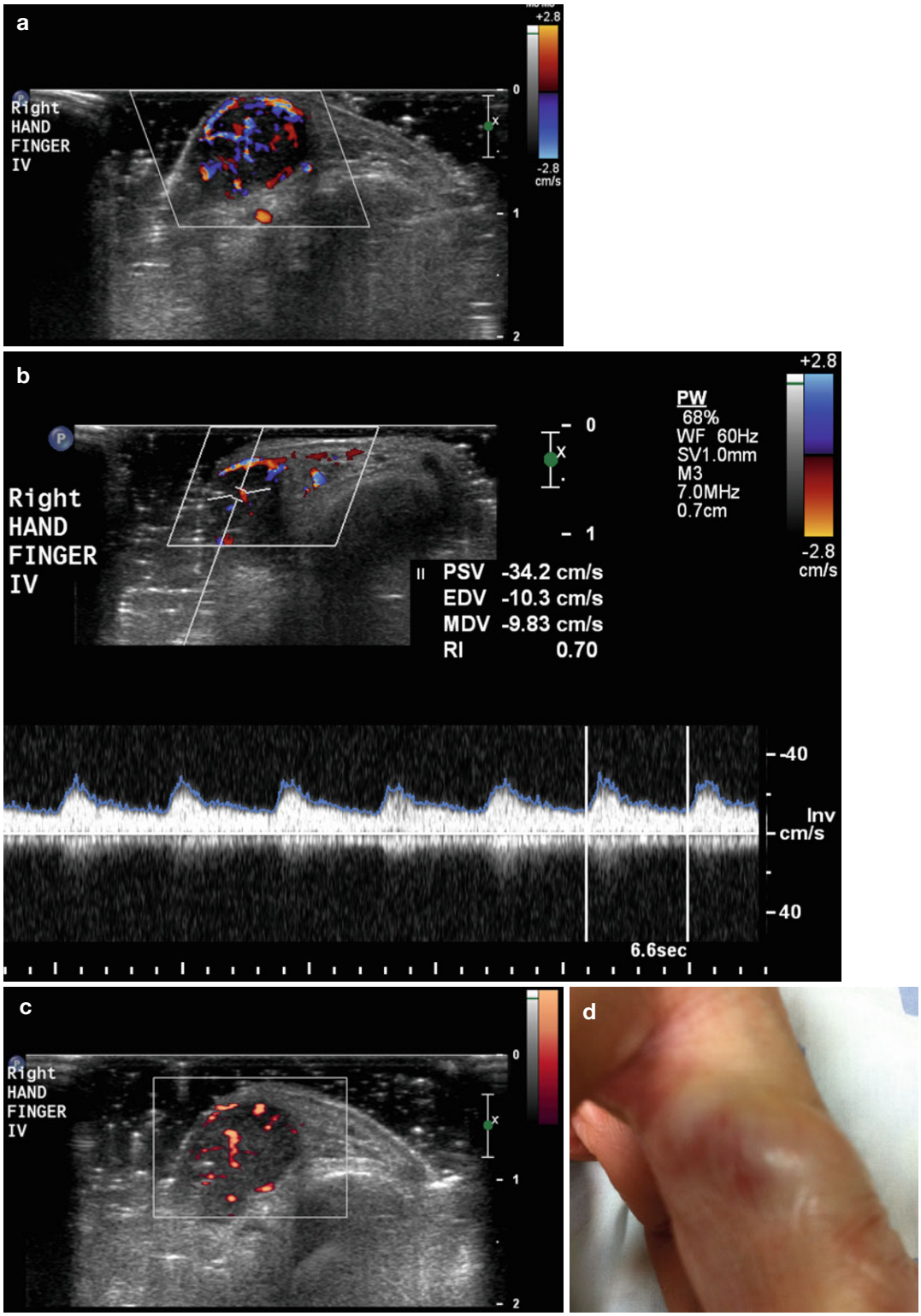

Fig. 1.11 Flow information provided by Doppler sonography. (**a**) Color Doppler flow. A rich vascularized lesion at the base of the right fourth hand finger, compatible with a vascular malformation is shown. Flowing blood is displayed in a color map, superimposed on the gray-scale image in real time. Flow direction: *red* toward the transducer and *blue* away from the transducer (see the *color bar* shown on the right side of the image), and relative velocity information (*lighter hues* corresponding to higher velocities) are provided. (**b**) Doppler frequency spectrum. Changes in flow velocity and flow direction are shown by vertical deflections of the waveform above the baseline. Doppler parameters are calculated: *PSV* (peak systolic velocity):34.2 cm/s; *EDV* (end diastolic velocity): 10.3 cm/s; *MDV* (mean blood flow velocity): 9.8 cm/s and *RI* (resistive index):0.70. (**c**) Power Doppler mode. Power flow uses a single color map to display the amplitude of the Doppler signals. Increased sensitivity for flow detection at lower velocities is achieved, although it lacks information on flow direction and flow velocity. (**d**) Anatomic picture of the lesion. A skin lump with skin redness is shown at the proximal fourth finger phalanx

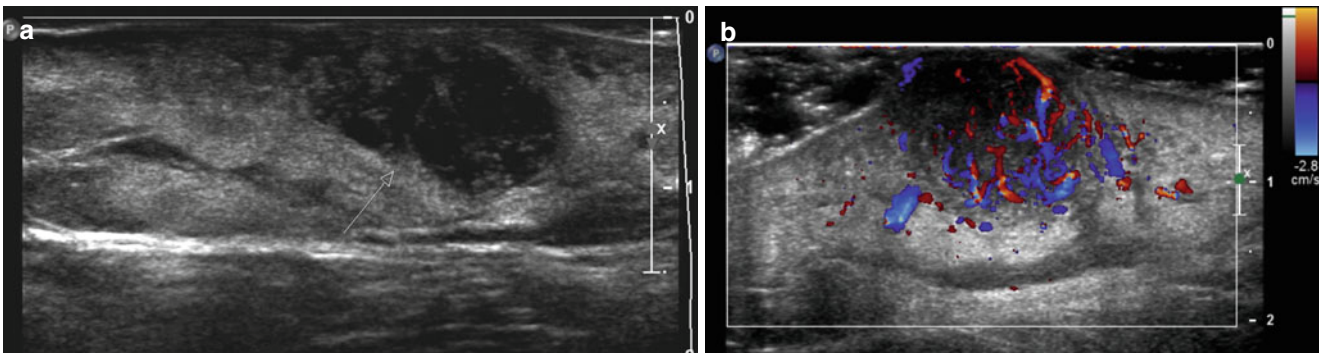

Fig. 1.12 Color Doppler sonography. Hypervascular lesion in the skin at the middle thigh, proved to be a dermatofibrosarcoma on histology. (**a**) On gray scale image, the tumor (*arrow*) is highly hypoechogenic and poorly delimitated. Hyperechogenic tissue surrounding the tumor represents edema in the subcutaneous fat. (**b**) Color Doppler shows a rich vascularity of the lesion

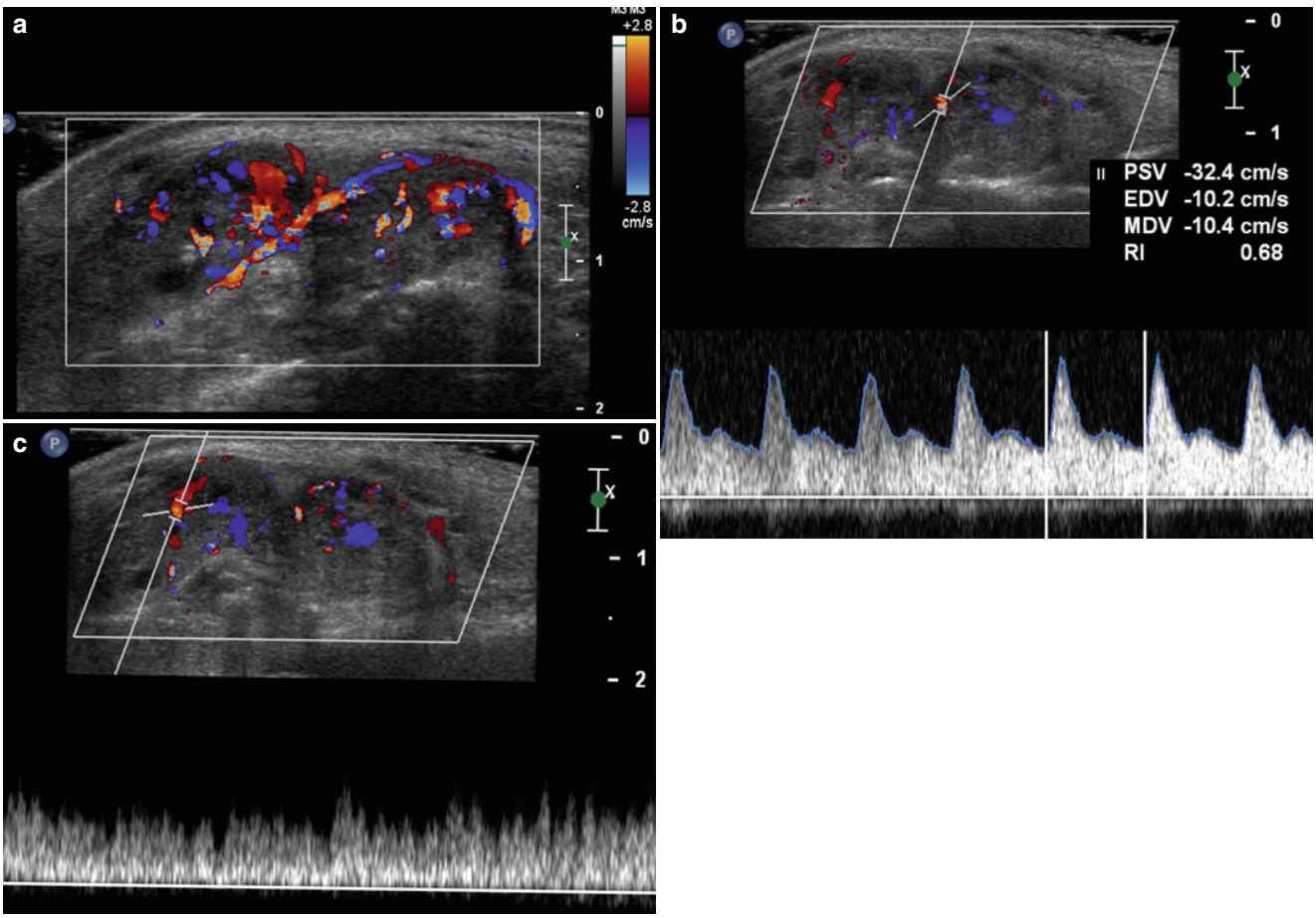

Fig. 1.13 Color and spectral Doppler sonography. A superficial hypervascular lesion at the dorsal left foot is shown. (**a**) Color Doppler display of vessels and flow direction. (**b**) Spectral Doppler display of arterial flow. Flow is displayed by placing the cursor (two parallel lines) into the vessel. Systolic, diastolic, and mean velocities are measured and resistive index calculated and displayed during one cardiac cycle (enclosed between the vertical lines on the spectral display, at the *bottom* of the image). (**c**) Spectral Doppler display of venous flow. Note that in this vein, flow direction is toward the transducer and as so, displayed in red and above the base line. Spectral Doppler allows differentiation between arterial and venous flow based on flow characteristics and flow velocities measurements

nail lesions. Wortsman et al. described glomus tumor of the nails evaluated with high-resolution color Doppler ultrasound using a compact linear probe 7–15 MHz in frequency [11]. The tumors appeared as hypoechoic nodules with high vascularity in the nail bed and remodeling of the underlying bone. Small tumors of 0.9 mm diameter could be identified and arterial flow was demonstrated in all tumors, with a varied peak systolic velocity, mean 11.3 ± 9.1 cm/s

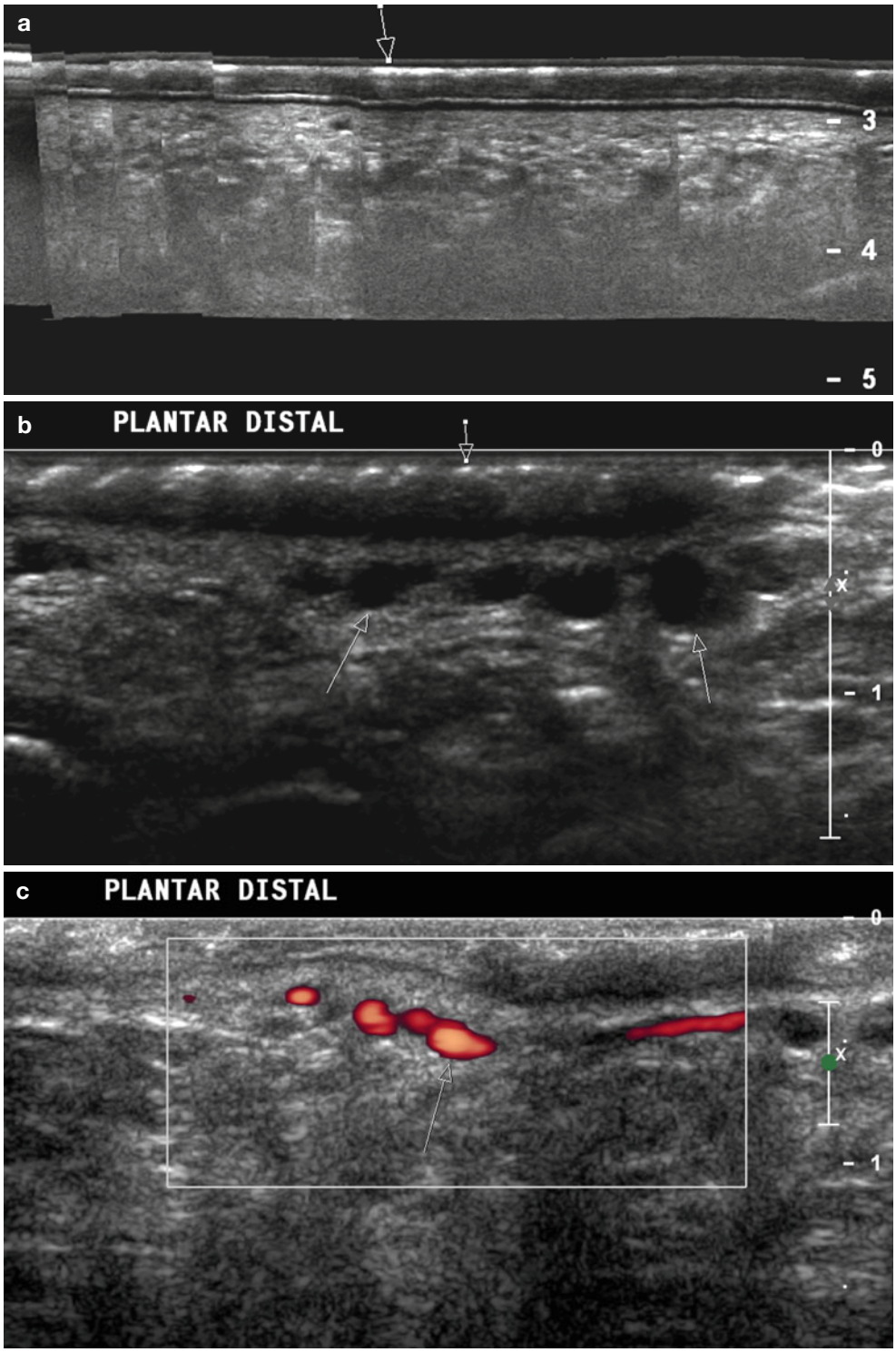

Fig. 1.14 Gray scale and color Doppler. Patient suffering from pachyonychia congenita, a rare autosomal dominant skin disorder characterized by hyperkeratosis on hands and feet. (**a**) Panoramic (EFOV) image performed over the blisters on the plantar foot. Hyperechoic (*white*) *dots* and *lines* are seen in the epidermis, representing hyperkeratosis (*arrow*). The anechoic layer interposed between the epidermis and the dermis is a result of water contained in the blisters. (**b**) Hyperechoic epidermis (*vertical short arrow*) and engorged varicose veins seen in the dermis as anechoic (*black*) dots (*oblique long arrows*). (**c**) Power Doppler sonography shows flow into the veins (*arrow*)

(range: 3.7–26.1 cm/s) Characteristic ultrasound pictures can be seen in psoriasis, cysts, vascular abnormalities, and other nail diseases [12]. Giovagnorio et al. described the ultrasound characteristics of 68 lesions suspicious of skin metastases [13]. Each nodule was classified by measurement of fundamental sonographic parameters- major diameter, shape, borders, echo texture, and homogeneity and by assessment of vascularity with color Doppler sonography - presence or absence of flow and vascular pattern. Of 68 nodules, 23 were malignant (21 metastases and 2 B-cell lymphomas), and 45 were benign (22 sebaceous cysts, 18 granulomas of different origins, 3 fibromas, and 2 neurofibromas). The nodules were localized in the subcutaneous space, had clearly demarcated borders, and were

hypoechoic. A circular or oval shape was predominant, but seven metastases had an irregular, polycyclic shape. On color Doppler sonography, none of the benign nodules or B-cell lymphomas showed signs of vascularity, whereas the metastatic nodules were all vascularized, with one or more peripheral poles (21 of 21 nodules) and internal vessels (11 of 21 nodules). A polycyclic shape and hypervascularity, with multiple peripheral poles and, eventually, internal vessels, should be considered the most indicative signs of metastasis. In a previous publication, 71 visible and palpable nodules of the skin and subcutaneous tissue were evaluated with color Doppler sonography [14]. The nodules were classified as avascular (type I), hypovascular with a single vascular pole (type II), hypervascular with multiple peripheral poles (type III), and hypervascular with internal vessels (type IV). Of the 32 malignant nodules, 9 % showed a type I pattern, 50 % had a type III pattern, and 41 % had a type IV pattern; of the 39 benign nodules, 86 % showed a type I pattern and 14 % had a type II pattern. The sensitivity and specificity of hypervascularity in malignant lesions were 90 and 100 % respectively; the sensitivity and specificity of hypovascularity in benign lesions were 100 and 90 % respectively. The authors conclude that color Doppler sonography is able to increase the specificity of ultrasonography in the evaluation of skin nodular lesions.

Benign tumors are associated with hyperemia and ectasia of the vessels but not with any appreciable formation of new vessels. It is well documented that many different kinds of malignant tumors are accompanied by angiogenesis. This vascularization is an important indicator of development and prognosis. The detection of Doppler signals is a simple, noninvasive method of analyzing this vascularization. Knowledge of the intratumoral vascularity can have an influence on the therapy, with regard to the extent of excision. Extensive vascularity in a primary tumor is probably an adverse prognostic factor for the possibility of early spread although, may be a good prognostic factor for chemotherapy treatment.

Hypervascularization is found both in inflammatory and malignant lesions at Doppler ultrasound examination of skin lesions, making difficult to differentiate between them. The introduction of *microbubble contrast injection for ultrasound* (*CEUS*) (Fig. 1.15) redefined the role of ultrasound in resolving vascular questions [15, 16]. CEUS can help delineate small vascular structures (0.1–0.3 mm in diameter) and enhance Doppler signals from low velocity small volumes of blood. Schroder et al. described the use of ultrasound contrast media for characterizing vascularization of benign and malignant skin tumors on enhanced color Doppler [15]. B-mode gray scale parameters such as tumor diameter, margins and echogenicity were evaluated. On color Doppler mode, rhythmically pulsating colored pixels corresponded to arterial vessels, which were confirmed by registering their Doppler spectrum. Afterwards, the mode was changed to the power Doppler mode without changing the technical settings. In most cases, the amplification had to be degraded to avoid confluence of the colored areas. Following conventional imaging, a signal-enhancing agent was intravenously injected. The main criterion of malignancy was the degree of the intratumoral vascularity as measured by the percentage vessel area (p.v.a.) of the lesions. The p.v.a. was defined as the ratio of colored intratumoral vessel areas to the other "gray" parts of the tumor. A significant difference was found between malignant and benign tumors ($p = 0.01$) with regard to the degree of vascularity. The mean p.v.a. of malignant tumors was 9.6 % before and 18.8 % on CEUS. The mean p.v.a. of benign tumors was 1.1 and 3.3 %, respectively. B-mode criteria - echogenicity, homogeneity, sharpness of the borders-and the calculated spectral Doppler values did not contribute to the differential diagnosis of the tumors. Analysis of tumor vascularity using the p.v.a. after injection of the signal enhancer was superior to B-mode, spectral Doppler ultrasound, and flow indices.

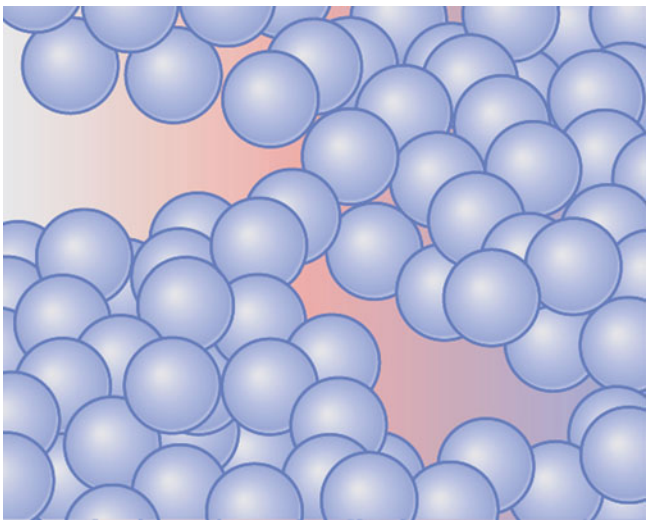

Fig. 1.15 Microbubbles for contrast enhancement in ultrasound imaging (*CEUS*). Encapsulated bubbles of gas, smaller than red blood cells. Intravascular agents capable of circulating freely (blood-pool agents), help delinate small vascular structures (0.1–0.3 mm in diameter) and enhance Doppler signals from low velocity small volumes of blood

Non-invasive preclinical imaging has evolved during the last decade for longitudinal studies of normal development and models of human disease in small animals [17]. High frequency 'micro-ultrasound' has steadily evolved in the post-genomic era. The upper limits of linear and phased arrays transducers have been pushed from about 20 to over 50 MHz enabling a broad range of new applications. Available imaging options are non- linear contrast agent imaging for relative vascularity and perfusion quantification (Fig. 1.16) and 3D imaging for anatomical and vascular

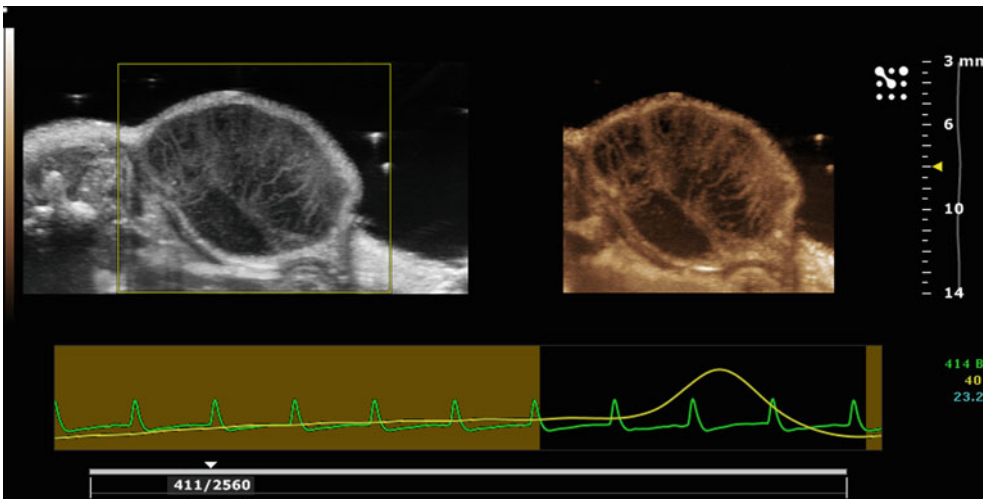

Fig. 1.16 Contrast enhancement in micro-ultrasound imaging. Tumor vascularization in a mouse tumor. Imaging is performed with a Vevo 2100 scanner using nonlinear contrast mode at 18 MHz. Wash-in of microbubble contrast agent (Vevo MicroMarker) following bolus injection in a tail vein. Ultrasound contrast agents are comprised of gas bubbles less than 5 μm in diameter encapsulated by a polymer or lipid shell. Signal acquisition is respiratory gated as shown in the image at the bottom of the picture. Tumor signals are suppressed by the nonlinear processing, leaving only the outline of the tumor. A branching pattern of vasculature is seen in the tumor, with a heterogeneous distribution

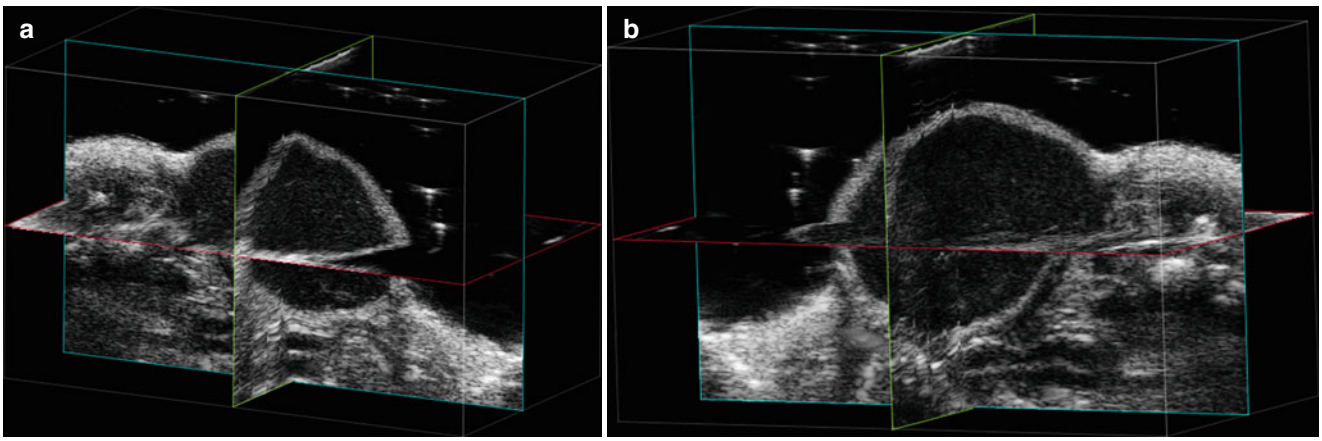

Fig. 1.17 3D-Mode imaging. (**a**, **b**) 3D images of a mouse tumor using a high frequency high resolution (30 μ resolution) linear array transducer (Vevo 2100 Imagin System. VisualSonics, Toronto). The intersecting planes can be displayed in arbitrary directions. Images can also be displayed as separate planes. 3D imaging combined with either B-Mode, Power Doppler Mode, or Nonlinear Contrast Imaging allows for quantification of volume and vascularity within a defined anatomical structure

visualization-when combined with power Doppler or contrast imaging- and volume and vascularity quantification (Fig. 1.17). Micro-ultrasound is playing an increasing role in preclinical studies and efforts are already underway to use the technology in clinical applications such as prostate, neonatal, ocular and skin imaging [18].

Tips and Teaching Points

1. High variable-frequency ultrasound transducers (HVFUS) 6–18 MHz with Doppler capability clearly define skin layers and deeper structures, and may show vascularization patterns and flow velocity.
2. Higher frequency transducers allow better resolution (as low as 0.1 mm), although the penetration depth decreases (6 mm depth at 20 MHz).
3. Power Doppler is more sensitive for low velocity flow, an thus better for poorly vascularized or low velocity flow lesions in the skin. No information on flow direction or flow velocity is provided.
4. Ultrasound examination is largely operator-dependent. It is advised to apply a large amount of gel over the skin and avoid compression with the transducer. Optimal adjustment of B-mode and Doppler technical settings must be made while performing US scans.

Conclusion

High-resolution gray scale sonography with color and spectral Doppler is a real-time noninvasive imaging technique that can be used as an adjunct to the clinical evaluation of skin and nail lesions. Superficial foreign bodies and hair fragments are easily identified. The procedure does not require administration of intravenous contrast media and provides good information about lesion characteristics and blood flow as well as surrounding structure invasion. Preoperative imaging aids in surgical planning by identifying the anatomical location and extent of a neoplasm and the presence of subclinical satellite lesions. Layers of involvement and vascularity patterns can be recognized in a non-invasive way. Measurements in ultrasound images have a good correlation with pathology. Sonographic monitoring of disease changes following medical treatment allows an objective verification of results and adjustment of treatment if necessary. Ultrasound may have a role in the evaluation of surgical treatment of skin lesions, allowing monitoring of therapeutic response, especially in suspicion of recurrence and in cases with persistent pain. Micro-ultrasound evolved in the last decade as a useful technique for preclinical studies and efforts are already under way for using it in clinical applications such as skin imaging.

Ultrasound is widely available and non-invasive and may therefore be used for longitudinal studies of skin lesions.

There are few limitations of the ultrasound technique, related mostly to its lack of sensitivity in detecting lesions localized to the epidermis or extremely thin (<0.1 mm) lesions, including port wine capillary vascular malformations and pigment deposits (melanin deposits), although epidermal thickening can be detected and can be particularly prominent in inflammatory or infectious conditions such as plantar warts.

Ultrasound examination is largely operator dependent. Optimal adjustment of B-mode and Doppler technical settings must be made while performing skin ultrasound.

Acknowledgment Edith Suss-Toby, Ph.D. and Michal Schlesinger-Lau, VMD, Imaging & Microscopy Unit, Multidisciplinary Laboratories, Faculty of Medicine, Technion, Israel Institute of Technology, Haifa, Israel, for the images on micro-ultrasound for preclinical imaging.

Glossary

Transducer Device that converts one form of energy into another. In ultrasound, the transducer converts electric energy provided by the transmitter to mechanical energy (acoustic pulses) and vice versa, reflected echoes to electric signals. Ultrasound transducers are made of thin piezoelectric materials that expand and contract to generate acoustic vibrations (frequencies).

Resolution Capacity to separate two objects in close proximity that are along the path of the ultrasound beam. Axial resolution is the smallest thickness while lateral resolution is the smallest width that can be resolved. Higher ultrasound frequencies raise the spatial resolution but lower the depth of penetration into the tissues.

Artifacts Source of imaging pitfalls, suggesting the presence of structures that are not actually present or obscuring real findings. Examples of artifacts suggesting structures that are not actually present are reverberation, refraction, and side lobes artifacts. Reverberation artifacts are a result of repeated reflection of the ultrasound signal between highly reflective interfaces usually near the transducer. Refraction artifacts are a result of bending of the sound beam causing targets that are not situated along the axis of the transducer to appear in a misleading location. Side lobes artifacts result from a strong out-of-plane reflector, generating confusing echoes. An example of artifact-obscuring findings is posterior acoustic shadowing. Acoustic shadow is a result of total reflection of the ultrasound waves by a strong reflector, causing loss of information on the tissues deep to the reflecting structure.

Harmonics Multiples or harmonic echoes of the transmitted fundamental frequency generated by the acoustic pulse as it travels within tissues.

Compounding Image resulting from summing ultrasound images obtained from different scanning angles.

Extended field of view (EFOV) Panoramic image generated by manual movement of a real-time probe in the direction of the transducer array. Imaging processing technology estimates translation and rotation of the probe by comparing successive images. The EFOV image buffer combines the images to produce a panoramic image.

3D Ultrasound Tissue volume acquired by dedicated 3D transducers employing hardware-based image registration, high density 2D arrays or software registration of scan planes.

Hypoechoic Reflected signals (echoes) of intermediate intensity or amplitude, generating images of low brightness in different shades of gray. Examples of hypoechoic tissues are the parenchymal organs such as the liver, spleen, renal parenchyma, and muscles.

Hyperechoic Reflected signals (echoes) of high intensity or amplitude, generating images of high brightness (white). Examples of hyperechoic tissues are fat, fibrous tissues, and bones. Foreign bodies and stones are examples of hyperechoic structures.

Echofree, sonolucent, or anechoic Absence of reflected signals (echoes), generating images in black. Examples of anechoic targets are normal vessels, gallbladder, urinary bladder, and cysts.

Doppler effect The result of the change in frequency of the sound when scattered by a moving target. The Doppler frequency shift is described by the Doppler equation:

$$\Delta F = (\mathrm{FR} - \mathrm{FT}) = (2\ \mathrm{FT}\ v / c)\cos\theta.$$

ΔF: Doppler frequency shift
FR: frequency of sound reflected from the moving target
FT: frequency of sound emitted from the transducer
v; target velocity
c: sound velocity in the medium
θ: angle between the flow axis and the incident ultrasound beam (angle of insonation). This angle must be kept at 60° or less.

Pulsatility index (PI) PI considers the tissue resistance to flow at each complete cardiac cycle. It is calculated as PI = PSV – EDV/mean velocity.

Resistive index (RI) RI considers the tissue resistance to blood flow at systole and diastole. It is calculated as RI = PSV – EDV/PSV

Contrast enhanced ultrasound agents (CEUS) Intravascular blood-pool agents comprised of encapsulated microbubbles of gas, smaller than red blood cells, capable of circulating freely. CEUS seek to enhance the echo amplitude by increasing the backscatter from moving red cells, while increasing attenuation from the static tissue.

References

1. Merrit CRB. Physics of ultrasound. In: Rumack CM, editor. Diagnostic ultrasound. 3rd ed. Philadelphia: Elsevier; 2005. p. 3–34.
2. Wortsman X, Wortsman J. Clinical usefulness of variable-frequency ultrasound in localized lesions of the skin. J Am Acad Dermatol. 2010;62:247–56.
3. Lassau N, Spatz A, Avril MF, et al. Value of high-frequency US for preoperative assessment of skin tumors. Radiographics. 1997;17:1559–651.
4. Cammarota T, Pinto F, Magliaro A, Sarno A. Current uses of diagnostic high-frequency US in dermatology. Eur J Radiol. 1998;27:215–23.
5. Szyman'ska E, Nowicki A, Mlosek K, et al. Skin imaging with high frequency ultrasound: preliminary results. Eur J Ultrasound. 2000;12:9–16.
6. Gerger A, Hofmann-Wellenhof R, Samonigg H, Smolle J. In vivo confocal laser scanning microscopy in the diagnosis of melanocytic skin tumors. Br J Dermatol. 2009;160:475–81.
7. Antoch G, Vogt FM, Freudenberg LS, Nazaradeh F, Goehde SC, Barkhausen J, et al. Whole-body dual-modality PET/CT and whole-body MRI for tumor staging in oncology. JAMA. 2003;290:3199–206.
8. Wortsman XC, Holm EA, Wulf HC, Jemec GBE. Real-time spatial compound ultrasound imaging of skin. Skin Res Technol. 2004;10:23–31.
9. Weng L, Tirumalai AP, Lowery CM, et al. US extended-field-of-view imaging technology. Radiology. 1997;203:877–80.
10. Hildegard Schmid-Wendtner M, Burgdorf W. Ultrasound scanning in dermatology. Arch Dermatol. 2005;14:217–24.
11. Wortsman X, Wortsman J, Soto R, et al. Benign tumors and pseudotumors of the nail: a novel application of sonography. J Ultrasound Med. 2010;29:803–16.
12. Gutierrez M, Wortsman X, Filippucci E, et al. High-frequency sonography in the evaluation of psoriasis: nail and skin involvement. J Ultrasound Med. 2009;28:1569–74.
13. Giovagnorio F, Valentini C, Paonessa A. High-resolution and color Doppler sonography in the evaluation of skin metastases. J Ultrasound Med. 2003;22:1017–22, quiz 1023–5.
14. Giovagnorio F, Andreoli C, De Cicco ML. Color Doppler sonography of focal lesions of the skin and subcutaneous tissue. J Ultrasound Med. 1999;18:89–93.
15. Schroder RJ, Maurer J, Zlowodski M, et al. Vascularization of malignant and benign skin tumors measured by D-galactose-based signal enhanced colour Doppler sonography. Acta Radiol. 2001;42:294–301.
16. Burns PN. Physics of ultrasound. In: Rumack CM, editor. Diagnostic ultrasound. 3rd ed. Philadelphia: Elsevier; 2005. p. 55–73.
17. Foster FS, Mehi J, Lukacs M, et al. A new 15–50 MHz array-based micro-ultrasound scanner for preclinical imaging. Ultrasound Med Biol. 2009;35:1700–8.
18. Foster FS, Hossack J, Lee Adamson S. Micro-ultrasound for preclinical imaging. Interface Focus. 2011;1:576–601.